RSC Advances

ROYAL SOCIETY OF CHEMISTRY

www.rsc.org/advances

Synthesis and characterization of polyamide thin film composite membrane based on polydopamine coated support layer for forward osmosis

Yangbo Huang, Haiyang Jin, Hao Li, Ping Yu*, Yunbai Luo
College of Chemistry and Molecular Sciences, Wuhan University, Wuhan 430072, Hubei, People's Republic of China
*Correspondence author: yuping@whu.edu.cn, +86-27-68752511 (P. Yu);
bobo180899@whu.edu.cn, +8613659834359 (Y. Huang);
haiyang@whu.edu.cn, +8613667151729 (H. Jin);
haol@whu.edu.cn, +8618064111112(H. Li)
ybai@whu.edu.cn, +8613807148090 (Y. Luo).

Abstract

In this study, a facile method has been developed to prepare high performance thin film composite (TFC) forward osmosis (FO) membranes, which was conducted by coating the surface of polysulfone (PSf) substrate with polydopamine (PDA) prior to the interfacial polymerization of trimesoyl chloride and m-phenylenediamine. The PDA coating layer was investigated by ATR-FTIR, XPS, FESEM and contact angle measurement. Results showed that the PDA layer played the following roles: (1) endowing the PSf substrate with catechol and ethylamino groups to enhance the hydrophilcity, which resulted in a significant increase in water flux; (2) facilitating the formation of a denser selective polydopamine layer during the interfacial polymerization process to enhance the salt rejection. The TFC membrane based on PDA coated dual PSf surfaces showed a water flux of 43.4 LMH and a salt flux of 6.46 gMH in pressure retarded osmosis (PRO) mode using 2 M NaCl as draw solution.

Keywords: Forward osmosis, Thin-film composite membrane, Surface modification, Polysulfone, Polydopamine

1. Introduction

Fresh water and energy shortage due to population growth is one of the major problems faced by humanity today. Recent researches on seawater desalination have focused on developing low energy consumption membrane separation processes. Forward osmosis (FO) is a novel membrane separation technology that utilizes osmotic pressure difference between the feed solution (FS) and the draw solution (DS) to force water across a semipermeable membrane. Compared to conventional hydraulic driven processes like nanofiltration (NF) and reverse osmosis (RO), FO

displays higher water recovery, better fouling resistance and less energy input.[1-4] Owing to these unique advantages, FO technology has received various interesting potential applications such as seawater desalination,[5-7] wastewater treatment,[8-9] food processing[10-11] and power generation.[12-13]

However，there are some technological obstacles that limit the advancement of FO process. One of the major challenges is to improve the FO membrane performance.[14] An ideal FO membrane should have the properties of high water permeability, high salt rejection and good chemical and thermal stability.[15,16] The current commercially available membranes made up of cellulose triacetate by Hydration Technologies Inc. show relatively low water flux, poor salt rejection and easy hydrolysis.[16-18] In this regard, over recent years many efforts have been made to develop thin film composite (TFC) FO membranes with a very thin skin layer and a porous support layer. However, the existence of internal concentration polarization (ICP) happened within the support layer limits the performance of these TFC membranes.[19] ICP is an exclusive phenomenon to FO process that significantly reduces the osmotic pressure gradient across the membrane and results in a decrease of the water flux.[20,21] There are two types of ICP due to the asymmetric FO membrane structure. A concentrative ICP occurs when the selective layer faces the draw solution (namely pressure retarded osmosis or PRO mode) as a result of salt accumulation inside the support layer. And a dilutive ICP happens due to the draw solution dilution in the substrate when the selective layer is placed towards the feed solution (namely FO mode).[14,18] According to the relevant literature, FO researchers generally agree that a promising substrate of TFC FO membrane should be porous, hydrophilic, thin as possible and low tortuosity to minimize the effect of ICP.[14,17,22] In recent years, many methods have been tried to improve the performance of PSf substrate. Y.H. La's group prepared TFC polyamide membranes on mesh-reinforced PSf supports which enabled a reduction in membrane thickness while maintaining good mechanical properties.[23] Y.H. Cho et al. fabricated a carboxylated PSf support layer for FO processes and this hydrophilic modification of FO membranes led to a dramatically higher water permeability compared to the conventional TFC polyamide membranes.[24] Several studies reported that nanoparticles could be embedded into the PSf substrate to prepare a novel nanocomposite membrane with a smaller structural parameter.[22,25,26]

In the past years, polydopamine (PDA), a mussel inspired polymer, has attracted much attention for membrane modification.[27-32] Owing to the catechol and ethylamino functional groups in dopamine (DA), a tightly adherent PDA layer can be easily created on the surfaces of many substrates such as polyvinylidene (PVDF), Polyethersulfone(PES) and polysulfone (PSf) via self-polymerization in a weak alkaline condition.[33-34] Enlightened by this peculiar polymer, Y. Li et al. have successfully synthesized a nanofiltration membrane based on PDA modified PES support layer which showed good structural stability.[28] L. Zhu's group has investigated the fundamental surface properties of PDA-coated hydrophobic substrates. They found that the surface free energy and hyophilicity of the PDA modified substrates were enhanced dramatically.[27] J.T. Arena et al. coated the PSf support layers of commercial RO membranes with PDA to use for FO process[30] and H.K. Lee's group also provided a facile method of preparing PDA modified PES hollow fiber membrane for pressure retarded osmosis[31].

In this work, polyamide (PA) flat sheet TFC-FO membranes were fabricated using 1,3-phenylenediamine and trimesoyl chloride via interfacial polymerization method. Before the PA selective layer formed, polysulfone substrate was coated by PDA. Three kinds of PDA modified substrates were prepared in this work using the same procedure and designated as

PDA@ top PSf, PDA@ bottom PSf and PDA@ dual PSf, respectively, which are illustrated in Fig. 1. Our present work aims to investigate how the PDA coating layers affect the whole performance of the FO membrane, including (1) the effect of top surface PDA coating on formation of the subsequent selective layer and (2) the relationship between the PDA coating and the hydrophilcity, salt rejection and water permeability. More specifically, the PDA@ top PSf aims to enhance the salt rejection while the PDA@ bottom PSf is supposed to improve the water permeability of the composite membrane. Then both advantages could be combined to prepare a TFC PDA@ dual PSf membrane which could show high water flux without serious loss in salt rejection.

2. Experimental materials and methods

2.1 Materials

Polysulfone beads (PSf, molecular weight: 52,000, EV-501, Solvay Advanced Polymers) was used for fabricating the membrane substrates. 1-methyl-2-pyrrolidinone (NMP, ⩾99.0%) and polyvinylpyrrolidone (PVP K-30) purchased from Sinopharm Chemical Reagent Co. Ltd were used as the solvent and porogen, respectively. The dopamine hydrochloride (DA, ⩾98.5%) and Tris-HCl purchased from Shanghai Ryon Biological Technology CO. Ltd were employed to modify the substrates. 1,3-phenylenediamine (MPD, ⩾99.5%), trimesoyl chloride (TMC, ⩾ 98.0%) and n-hexane (⩾97.0%) purchased from Sinopharm Chemical Reagent Co., Ltd were used for interfacial polymerization. Sodium chloride (NaCl, ⩾99.5%) provided by Sinopharm Chemical Reagent Co. Ltd was dissolved in deionized water (DI, 8-10 μs/cm) for FO and RO tests.

2.2 Preparation of PSf membrane substrates

The PSf substrates were prepared via phase inversion method.[35] The casting solution was prepared by mixing Polysulfone beads (18 wt%) with NMP (81.5 wt%) as solvent and PVP (0.5 wt%) as porogen and stirred by a Yitong Electron mechanical stirrer at 70 □ for 5 hours. The polymer solution was then placed in a desiccator overnight to remove bubbles. The casting solution was casted on a dry glass plate with a 140 μm casting knife, followed by immersion into a water bath at room temperature immediately to induce phase inversion. After the membrane formation was finished, it was peeled off the glass plate and rinsed in a tap water bath to remove the residual solvent. Finally, the membrane was kept in DI bath before use.

2.3 Modification of PSf substrate with PDA

The surface modification steps took place in a custom-made coating frame which limited the coating solution to only one side of the substrate. The dopamine solution was prepared by dissolving 0.1 g dopamine hydrochloride in 50 mL of pH=8.5~ 8.8 tris-HCl buffer and it was quickly poured onto the membrane surface after it was ready. The reaction took place at 25 □ in air ambient conditions for 1 hour. After the coating was finished, the modified membrane was thoroughly rinsed by DI water to remove the residual chemicals. The membrane was then kept in DI bath before interfacial polymerization. Both the top and the bottom surface modification of the PSf substrate were performed in the same procedure and condition. Three kinds of PDA modified substrates were prepared in this work and they are illustrated in Fig. 1.

2.4 Fabrication of polyamide selective layer

The polyamide selective layer of TFC membrane was prepared on the top surface of the PSf substrate via interfacial polymerization process. At first, the substrate was immersed in 50 mL of 2 wt% MPD aqueous solution for 120 s. The excess MPD liquid droplet was swept off by a Whatman filter paper. Next, 50 mL of 0.1% (w/v) TMC n-hexane solution was poured onto the membrane surface and held on the substrate for 120 s to form a polyamide thin film. The resultant TFC membrane was then rinsed by DI water and kept in DI bath until use.

2.5 Membrane characterizations

The functional groups of polydopamine layer were identified by a Nicolet AVATAR 360 Attenuated total reflectance-Fourier transform infrared (ATR-FTIR) spectroscope. An ESCALAB 250Xi X-ray photoelectron spectroscopy (XPS, Thermo Fisher, USA) with a source gun type of Al Kα was employed to determine the chemical changes of the membrane surface with and without polydopamine modification. Membrane surface morphologies and roughness were examined with a field-emission scanning electron microscope (FESEM, Sigma, Zeiss) from Germany and an atomic force microscope (AFM, SPM-9500J3) from Shimadzu, respectively. Surface hydrophilicity was determined using a DSA 100 dynamic contact angle instrument from Germany.

2.6 Membrane performance tests

The permeability and selectivity of the FO membranes were tested in a customized lab-scale reserves osmosis unit.[36] The membrane cell has an effective area (A_m) of 46.5 cm^2. All tests were conducted at 25±0.5 □ and external concentration polarization was ignored because of a relatively high recirculation rate. In RO tests, the pure water flux (J_w) and water permeability (A) were measured over an operating pressure of 2.5 bar with DI water as feed solution. The J_w and A were calculated using Eqs. (1) and (2).

$$J_w = \frac{\Delta V}{A_m \Delta t} \quad (1)$$

$$A = \frac{J_w}{\Delta P} \quad (2)$$

where ΔV is the volume of permeate water collected over the operating time Δt and ΔP is the trans-membrane pressure. Salt rejection (R) and salt permeability (B) were evaluated using 20 mM NaCl as feed solution at a pressure of 2.5 bar. R can be expressed as:

$$R = (1 - \frac{C_p}{C_f}) \times 100\% \quad (3)$$

where C_f and C_p are the concentrations of feed solution and permeate solution, respectively. Both parameters were determined by an ICS-900 ion chromatography (Dionex, USA). Based on the pre-measured parameters of A and R, and the known values of hydraulic pressure difference ΔP and osmotic pressure difference $\Delta\pi$, Salt permeability can be calculated by Eqs. (4).

$$\frac{1-R}{R} = \frac{B}{A(\Delta P - \Delta\pi)} \quad (4)$$

FO performance of the prepared membranes was measured with a custom-make lab-scale FO setup which is illustrated in Fig. 2. The cross-flow membrane cell has an effective area of 22.37 cm^2. Pure water and concentrated NaCl solutions (1 M and 2 M) were used as feed solution and draw solution, respectively. Both solutions were circulated at a flow velocity of 15 L/h. The feed and draw solution were both 1 L and kept 25 □ during the tests. All of the FO membranes were tested in both PRO and FO modes. To minimize experimental error, every parameter was determined at least three times to get an average value.

The water flux (J_v) was evaluated by the weight increment in draw solution tank during the testing time interval.

$$J_v = \frac{\Delta m_{draw}}{A_m \Delta t} \quad (5)$$

where Δm_{draw} is the mass increment of draw solution and Δt is testing time interval.

The reverse salt flux (J_s) was measured by calculating the content increment of NaCl in feed solution in the period of testing time.

$$J_s = \frac{\Delta(C_f V_f)}{A_m \Delta t} \quad (6)$$

where C_f and V_f are the NaCl concentration and volume of feed solution at the end of test, respectively.

3 Results and discussion

3.1 Surface chemistry of PDA coating

Many researchers have reported that dopamine molecules would undergo oxidation and polymerization in a weak alkaline condition and adhere to membrane surface to form a thin PDA layer.[29,37] ATR-FTIR spectroscope was used to analyze the chemical structure of membrane surface. Fig. 3 shows the ATR-FTIR spectra of original PSf and PDA modified PSf membranes. It is obvious that two new absorption peaks appear in the PDA coated membrane. The peak at 1657 cm^{-1} was corresponding to the deformation vibration of N-H in polydopamine. Another new peak appears between 3100 and 3600 cm^{-1} was attributed to O-H and N-H stretching vibration.[27] These characteristic peaks proved that the PDA layer was successfully prepared on the PSf film.

Furthermore, XPS spectroscope was used to quantitatively analyze the surface element compositions of the pristine and modified membranes. The XPS wide scans are presented in Fig. 4 and the atomic percentage of membrane surface are illustrated in Table 1. Compared to the original PSf membrane, a nitrogen (N1s) signal appeared in the PDA@PSf membrane, which implies the successfully coating of PDA skin layer. Meanwhile, the peak intensity of S(2s) and S(2p) and element compositions were evidently different. As shown in table 1, the atomic percentage of S declined from 3.02% to 0.66%, and the C/N molar ratio for PDA@ top PSf membrane was 9.18, which was a bit larger than the theoretical value of pure dopamine (8.0). The results indicated that the thickness of PDA coated layer on the top surface of PSf was approximate

to the analysis deepness of XPS.

3.2 Morphology and structure of membrane substrates

Fig. 5 illustrates the surface morphology of the original and modified membranes. It is obvious that the color of membrane surfaces (both top and bottom) became dark brownish after the PDA coating. This result was consist with the reports in other literatures[34,38] and implied the formation of PDA layer. It was found that some nano-scale particles appeared on the surface of PDA coated substrates. This indicated that there were some aggregated nanoparticles of dopamine formed during the self-polymerization process. The similar phenomenon was observed by Cheng.[29] In addition, the hydrophilicity of PDA modified PSf was improved significantly . As presented in Fig. 5, the contact angle (CA) on the top surface of PSf decreased from 71.4° to 40.3° and the CA on the bottom of PSf decreased from 56.0° to 30.6° after being coated by PDA. This was mainly due to the hydrophilic groups in the PDA molecules.

The three-dimensional AFM images in Fig. 6 show that the pristine PSf membrane has a relative small square average roughness (*Rms*) of 8.0 nm, while the value of *Rms* increases to 21.1 nm after the PDA coating. As it was observed in Fig. 6, the surface morphology of PDA@top PSf substrate became much rougher and some irregular protuberance of PDA nanoparticles were found. These were coincident with the results of FESEM images. Generally, the PDA coated substrates showed different surface chemical properties, improved hydrophilicity and rougher surface compared to the pristine membrane. These improvements may have a big influence on the fabrication process of polyamide selective layer and affect the performance of the TFC FO membranes.

3.3 Characteristics of the TFC-FO membranes

AFM data summarized in table 2 shows that the surface roughness of membrane increased sharply after the formation of PA layer. Compared to the TFC PSf membrane, the PA layers formed on PDA surface have a rougher surface and the square average roughness (*Rms*) increased from 43.4 nm to about 60nm. Fig. 7 shows the surface morphology of TFC FO membranes with different substrates. The active PA layer displayed a continuous “ridge and valley” morphology which is a typical characteristic of TFC PA membranes. This active layer primarily determines the water flux and solute rejection of the resultant FO membrane. As shown in Fig. 7, the surface morphology of the TFC membrane and the TFC PDA@ top PSf are very different. This indicates that the PDA coating has a big influence on the subsequent interfacial polymerization as well as the salt rejection of the resultant FO membrane, which will be discussed in the next part. In addition, it can be seen from the cross-sectional FESEM images in Fig. 8 that the thickness of the skin layer of the original TFC membrane is nearly the same as the TFC membrane with a top PDA layer.

Table 3 presents the separation properties of membranes prepared with different substrates. It is reported that all of the PDA modified TFC FO membranes showed a better water permeability comparing to the pristine TFC FO membrane. This can be explained by the improved hydrophilicity of the substrates. We generally believe that water transporting a hydrophilic substrate encounters less mass transfer resistance than the unmodified PSf support layer. It is worth noting that the PDA modification on the bottom surface of PSf is more favorable to improve the water permeability. As shown in table 3, the water permeability of TFC PDA@ bottom PSf

membrane was 1.34 L/m^2 bar h while that of TFC PDA@ top PSf membrane was 1.19 L/m^2 bar h. These might be attributed to the following reasons. Firstly, both sides of the TFC PDA@ bottom PSf membrane (PA layer and PDA layer) were hydrophilic while the TFC PDA@ top PSf membrane only had one hydrophilic side (PA layer). Secondly, according to Arena's report, since there were relative big pores on the bottom surface of PSf (Fig. 4), dopamine could easily penetrated into the substrate and attached onto the inside pore walls, which could enhance the hydrophilicity and "wetted porosity".[32] However, although the TFC PDA@ bottom PSf membrane showed a remarkable increase in water permeability, its salt rejection decreased from 86.5% to 80.2%. For TFC PDA@ bottom PSf membrane, the water permeability and salt permeability showed a "trade-off relationship" which elucidated by previous research.[39] However, the TFC PDA@ top PSf membrane displayed a satisfactory performance in terms of NaCl rejection. The NaCl rejection increased from 86.5% to 89.2%. The results indicated that the PDA layer on the top surface might help to form a denser selective PA layer during the subsequent interfacial polymerization process. T.S. Chung's group[32] also reported that the amine remained in the PDA layer could react with trimesoyl chloride monomers which might result in a denser and more stable PA layer. In summary, the PDA coated on the bottom surface of PSf helped to enhance the water permeability while the PDA coated on the top surface of PSf mainly contributed to improvement of salt rejection. Therefore, the TFC PDA@ dual PSf membrane would be a good choice to achieve high water flux without sacrificing the salt rejection.

3.4 FO performance evaluation

Fig. 9 compares the water flux of TFC FO membranes prepared on pristine PSf and PDA modified PSf substrates using DI water as feed solution and either 1 M or 2 M NaCl as draw solution under both FO and PRO modes. The TFC PSf membrane displayed relative poor water fluxes as low as 6.4 LMH in FO mode and 12.0 LMH in PRO mode when 2 M NaCl was used as draw solution. But the good news was that the water flux increased significantly when the PSf substrate was coated by the PDA layer, and it reached the maximum value of 23.3 LMH in FO mode and 43.4 LMH in PRO mode for TFC PDA@ dual PSf membrane. These were mainly due to the improved hydrophilicity of substrate. In addition, Fig. 8 also shows that the water flux in FO mode was much lower than that of PRO mode because of serious ICP effect. The results also showed that a high water flux was achieved by employing draw solution in high concentration (i.e. 2 M NaCl) as it could provide stronger driving force across the membrane.

The solute fluxes of the four types of TFC FO membranes are shown in Fig. 10. A reduction in solute leakage was observed for TFC PDA@ top PSf membrane. The results proved that the PDA coated on the top surface of PSf had an positive effect on the subsequent interfacial polymerization reaction to form PA layer. However, the TFC PDA@ bottom PSf membrane showed a dramatical increase in salt flux . Generally, the key feature of an ideal FO membrane is low reverse salt flux in addition to high water flux. Fortunately, the resultant TFC PDA@ dual PSf membrane can achieve a high water flux without serious loss in salt rejection.

4 Conclusions

In this study, three kinds of thin film composite (TFC) membranes based on polydopamine coated support layers were successfully synthesized. Compared to the TFC PSf membrane, the

water permeability of all the modified membranes were significantly improved. The enhancement in water flux mainly owes to the improved hydrophilicity of the PSf substrates which facilitate water across the membrane and diminish ICP effect. Results also showed that the PDA coated on the top surface of the substrate changed the surface chemical properties and roughness, which had a positive effect on the formation of PA selective layer. The resultant TFC PDA@dual PSf membrane showed high water flux without serious loss in salt rejection, which meant that this newly developed FO membrane displayed great perspective in forward osmosis applications.

Acknowledgments

This work was supported by the Plan of the National Science and Technology Support Program (2012BAC02B03).

Reference

[1] D.L. Shaffer, J.R. Werber, H. Jaramillo, S. Lin and M. Elimelech, Forward osmosis: Where are we now? Desalination, 2015, 356, 271-284.

[2] A. Achilli, T.Y. Cath, E.A. Marchand and A.E. Childress, The forward osmosis membrane bioreactor: a low fouling alternative to MBR processes, Desalination, 2009, 239, 10–21.

[3] E.R. Cornelissen, D. Harmsen, K.F. de Korte, C.J. Ruiken, J.J. Qin and H. Oo, L.P. Wessels, Membrane fouling and process performance of forward osmosis membranes on activated sludge, J. Membr. Sci., 2008, 319, 158-168.

[4] R.L. McGinnis and M. Elimelech, Energy requirements of ammonia–carbon dioxide forward osmosis desalination, Desalination, 2007, 207, 370–382.

[5] S. Zhao, L. Zou, C.Y. Tang and D. Mulcahy, Recent developments in forward osmosis: opportunities and challenges, J. Membr. Sci., 2012, 396, 1-21.

[6] R.V. Linares, Z. Li, S. Sarp, S.S. Bucs and G. Amy, J.S. Vrouwenvelder, Forward osmosis niches in seawater desalination and wastewater reuse, Water Res., 2014, 66, 122-139.

[7] J.R. McCutcheon, R.L. McGinnis and M. Elimelech, Desalination by ammonia–carbon dioxide forward osmosis: influence of draw and feed solution concentrations on process performance, J. Membr. Sci., 2006, 278, 114-123.

[8] X. Zhang, Z. Ning, D.K. Wang and J.C.D. Costa, Processing municipal wastewaters by forward osmosis using CTA membrane, J. Membr. Sci., 2014, 468, 269-275.

[9] P. Liu, H. Zhang, Y. Feng, C. Shen and F. Yang, Integrating electrochemical oxidation into forward osmosis process for removal of trace antibiotics in wastewater, J. Hazard. Mater., 2015, 296, 248-255.

[10] E.M. Garcia-Castello, J.R. McCutcheon and M. Elimelech, Performance evaluation of sucrose concentration using forward osmosis, J. Membr. Sci., 2009, 338, 61–66.

[11] B. Jiao, A. Cassano and E. Drioli, Recent advances on membrane processes for the concentration of fruit juices: a review. J. Food Eng., 2004, 63, 303-324.

[12] E. Nagy, A general, resistance-in-series, salt- and water flux models for forward osmosis and pressure-retarded osmosis for energy generation, J. Membr. Sci., 2014, 460, 71-81.

[13] A. Altaee, G. Zaragoza and A. Sharif, Pressure retarded osmosis for power generation and seawater desalination: Performance analysis, Desalination, 2014,344, 108-115.

[14] J. Wei, C. Qiu, C.Y. Tang, R. Wang and A.G. Fane, Synthesis and characterization of flat-sheet thin film composite forward osmosis membranes, J. Membr. Sci., 2011, 372, 292-302.
[15] S.B. Kwon, J.S. Lee, S.J. Kwon, S.T. Yun, S. Lee and J.H. Lee, Molecular layer-by-layer assembled forward osmosis membranes, J. Membr. Sci., 2015, 488, 111-120.
[16] N.Y. Yip, A. Tiraferri, W.A. Phillip, J.D. Schiffman and M. Elimelech, High performance thin-film composite forward osmosis membrane, Environ. Sci. Technol., 2010, 44, 3812-3818.
[17] X. Liu and H.Y. Ng, Double-blade casting technique for optimizing substrate membrane in thin-film composite forward osmosis membrane fabrication, J. Membr. Sci., 2014, 469, 112-126.
[18] N. Navid, J. Mohsen and R. Ahmad, The effect of SiO2 nanoparticles on morphology and performance of thin film composite membranes for forward osmosis application, Desalination, 2014, 343, 140-146.
[19] A. Sotto, A. Rashed, R.X. Zhang, A. Martinez, L. Braken, P. Luis and B. Van der Bruggen, Improved membrane structures for seawater desalination by studying the influence of sublayers, Desalination, 2012, 287, 317–325.
[20] X.X. Song, Z.Y. Liu and D.D. Sun, Nano gives the answer: breaking the bottle neck of internal concentration polarization with a nano fiber composite forward osmosis membrane for a high water production rate, Adv.Mater., 2011, 23, 3256–3260.
[21] G.T. Gray, J.R. McCutcheon and M. Elimelech, Internal concentration polarization in forward osmosis: role of membrane orientation, Desalination, 2006, 197, 1-8.
[22] D. Emadzadeh, W.J. Lau and A.F. Ismail, Synthesis of thin film nanocomposite forward osmosis membrane with enhancement in water flux without sacrificing salt rejection, Desalination, 2013, 330, 90-99.
[23] D. Stillman, L. Krupp and Y.H. La, Mesh-reinforced thin film composite membranes for forward osmosis applications: The structure–performance relationship, J. Membr. Sci., 2014, 468, 308-316.
[24] Y.H. Cho, J. Han, S. Han, M.D. Guiver and H.B. Park, Polyamide thin-film composite membranes based on carboxylated polysulfone microporous support membranes for forward osmosis, J. Membr. Sci., 2013, 445, 220-227.
[25] X.K. Ma, N.H. Lee, H.J. Oh, J.S. Hwang and S.J. Kim, Preparation and characterization of silica/polyamide–amide nanocomposite thin films, Nanoscale Res. Lett., 2010, 5, 1846-1851.
[26] M. Pakizeh, A.N. Moghadam, M.R. Omidkhah and M. Namvar-Mahboub, Preparation and characterization of dimethyldichlorosilane modified SiO_2/PSf nanocomposite membrane, Korean J. Chem. Eng., 2013, 30, 751-760.
[27] J. Jiang, L. Zhu, L. Zhu, B. Zhu, Y. Xu and Surface characteristics of a self-polymerized dopamine coating deposited on hydrophobic polymer films. Langmuir, 2011, 27, 14180-14187.
[28] Y. Li, Y. Su, J. Li, X. Zhao, R. Zhang and X. Fan, Preparation of thin film composite nanofiltration membrane with improved structural stability through the mediation of polydopamine, J. Membr. Sci., 2015, 476, 10–19.
[29] C. Cheng, S. Li, W. Zhao, Q. Wei, S. Nie and S. Sun, The hydrodynamic permeability and surface property of polyethersulfone ultrafiltration membranes with mussel-inspired polydopamine coatings, J. Membr. Sci., 2012, 417, 228–236.
[30] J.T. Arena, B. Mccloskey, B.D. Freeman and J.R. Mccutcheon, Surface modification of thin film composite membrane support layers with polydopamine: enabling use of reverse osmosis membranes in pressure retarded osmosis, J. Membr. Sci., 2011, 375, 55–62.

[31] P.G. Ingole, W. Choi, K.H. Kim, C.H. Park, W.K. Choi and H.K. Lee, Synthesis, characterization and surface modification of PES hollow fiber membrane support with polydopamine and thin film composite for energy generation, Chem. Eng. J., 2014, 243, 137-146.

[32] F. Li, J. Ye, L. Yang, C. Deng, Q. Tian and B. Yang, Surface modification of ultrafiltration membranes by grafting glycine-functionalized pva based on polydopamine coatings, Appl. Surf. Sci., 2015, 345, 301 – 309.

[33] G. Han, S. Zhang, X. Li, N. Widjojo and T.S. Chung, Thin film composite forward osmosis membranes based on polydopamine modified polysulfone substrates with enhancements in both water flux and salt rejection, Chem. Eng. Sci., 2012, 80, 219–231.

[34] L. Shao, Z.X. Wang, Y.L. Zhang, Z.X. Jiang and Y.Y Liu, A facile strategy to enhance pvdf ultrafiltration membrane performance via self-polymerized polydopamine followed by hydrolysis of ammonium fluotitanate, J. Membr. Sci., 2014, 461, 10–21.

[35] A. Tiraferri, N.Y. Yip, W.A. Phillip, J.D. Schiffman and M. Elimelech, Relating performance of thin-film composite forward osmosis membranes to support layer formation and structure, J. Membr. Sci., 2011, 367, 340-352.

[36] H. Li, Y. Lin, P. Yu, Y. Lou and L. Hou, FTIR study of fatty acid fouling of reverse osmosis membranes: Effects of pH, ionic strength, calcium, magnesium and temperature, Sep. Purif. Technol., 2011, 77, 171-178.

[37]H. Lee, S.M. Dellatore, W.M. Miller and P.B. Messersmith, Mussel-inspired surface chemistry for multifunctional coatings, Science, 2007, 318, 426–430.

[38] F. Li, J. Meng, J. Ye, B. Yang, Q. Tian and C. Deng, Surface modification of PES ultrafiltration membrane by polydopamine coating and poly(ethylene glycol) grafting: morphology, stability, and anti-fouling, Desalination, 2014, 344, 422–430.

[39] G.M. Geise, H.B. Park, A.C. Sagle, B.D. Freeman and J.E. McGrath, Water permeability and water/salt selectivity tradeoff in polymers for desalination, J. Membr. Sci., 2011, 369, 130-138.

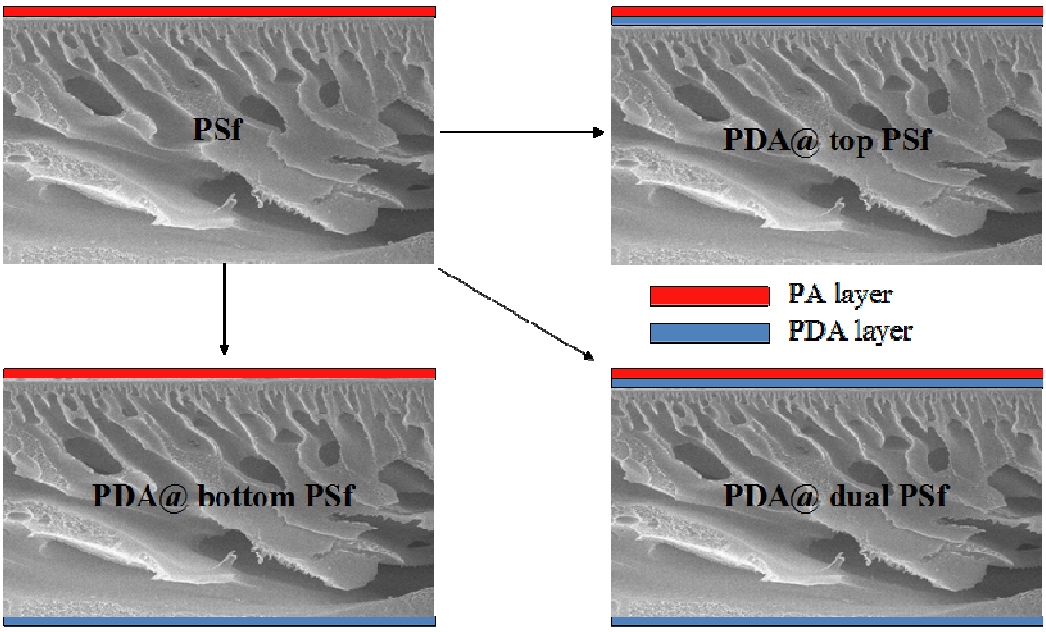

Figure 1 The illustration of four kinds of TFC FO membranes.

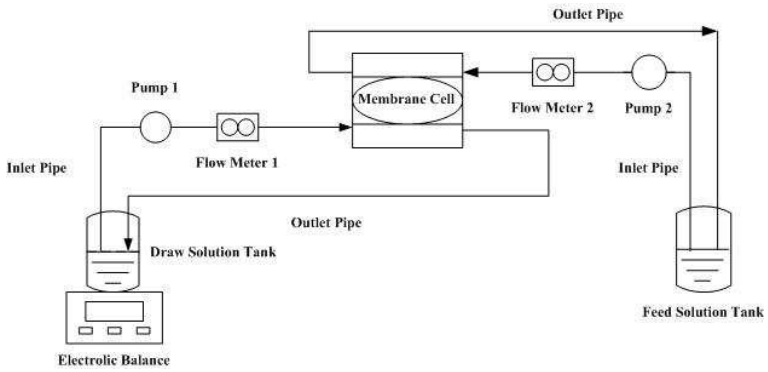

Figure 2 Set up of Lab-scale forward osmosis system

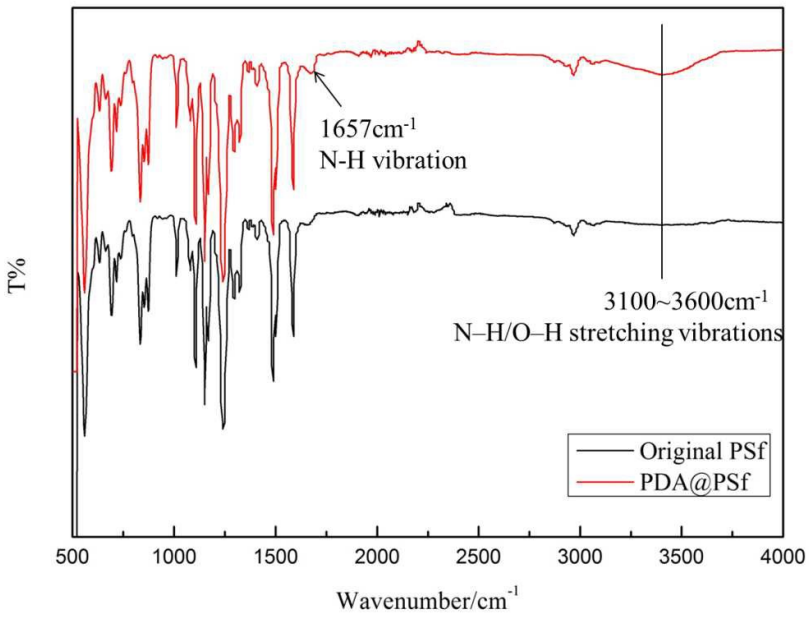

Figure 3 ATR-FTIR spectra of original PSf and PDA modified PSf membranes

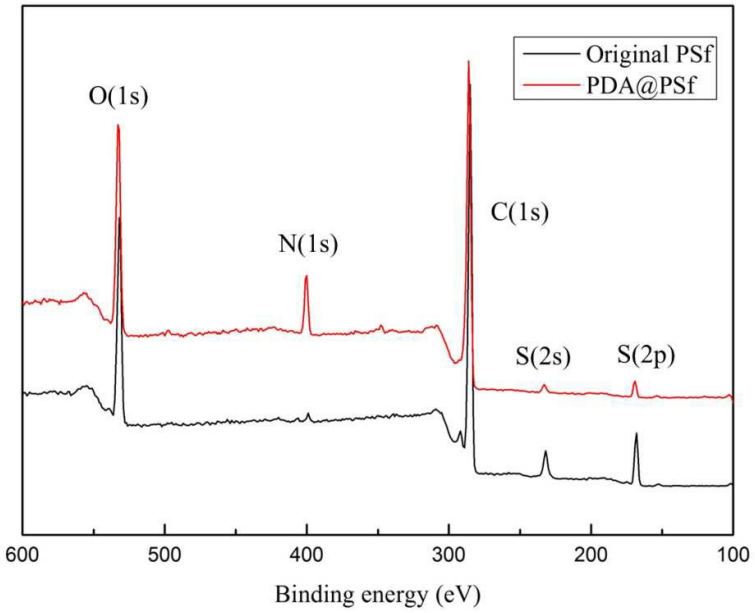

Figure 4 XPS spectra of original PSf and PDA coated PSf membranes.

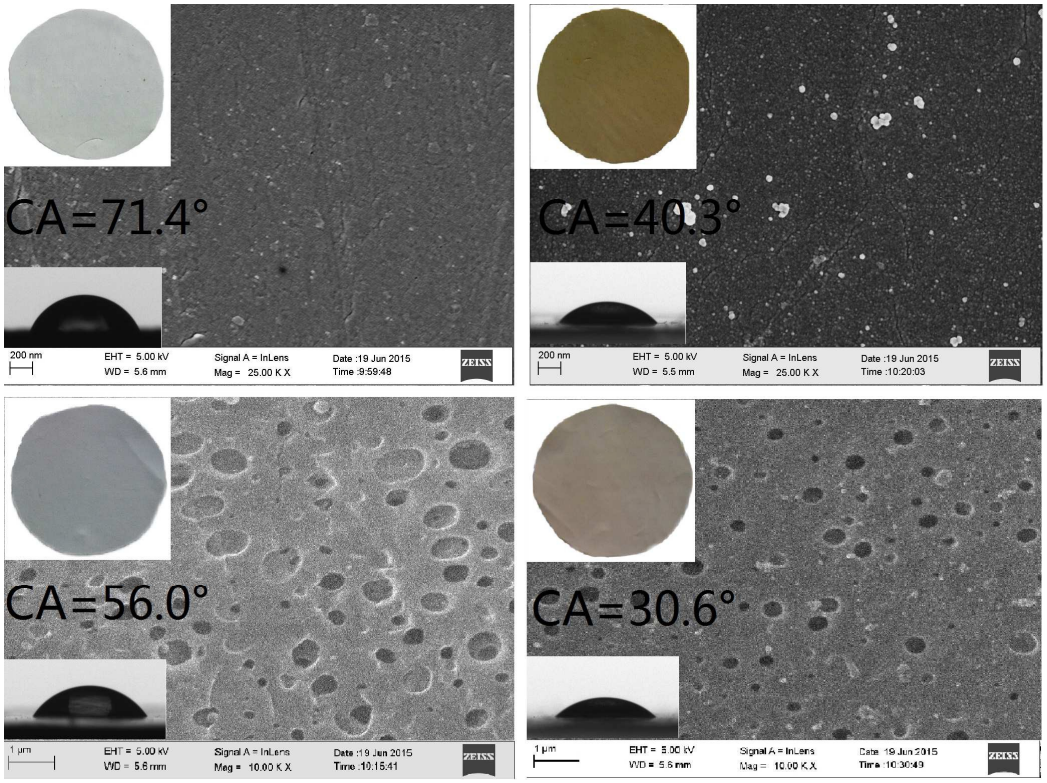

Figure 5 Photographs and FESEM images of the original PSf and PDA modified PSf membranes. (a) top surface of PSf, (b) top surface of PDA@ top PSf, (c) bottom surface of PSf, (d) bottom surface of PDA@ bottom PSf.

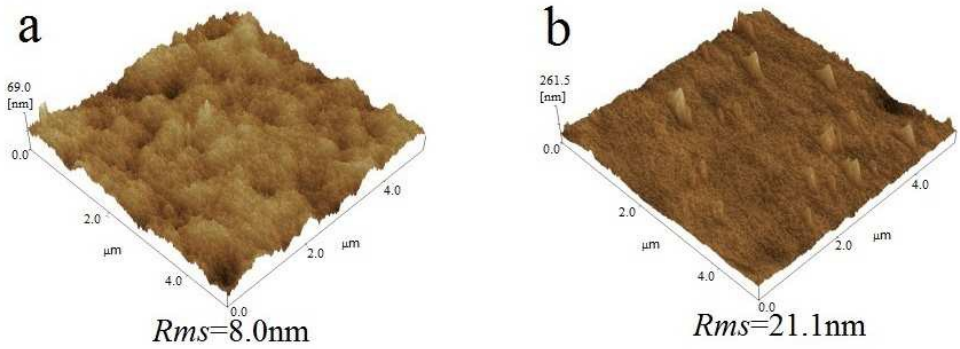

Figure 6 AFM images and square average roughness (*Rms*) for (a) PSf, (b) PDA@ top PSf.

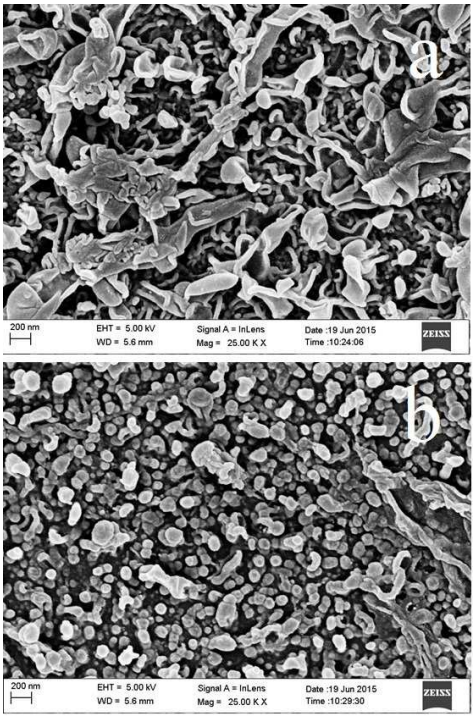

Figure 7 Surface FESEM images of (a) TFC PSf membrane, (b) TFC PDA@ top PSf membrane.

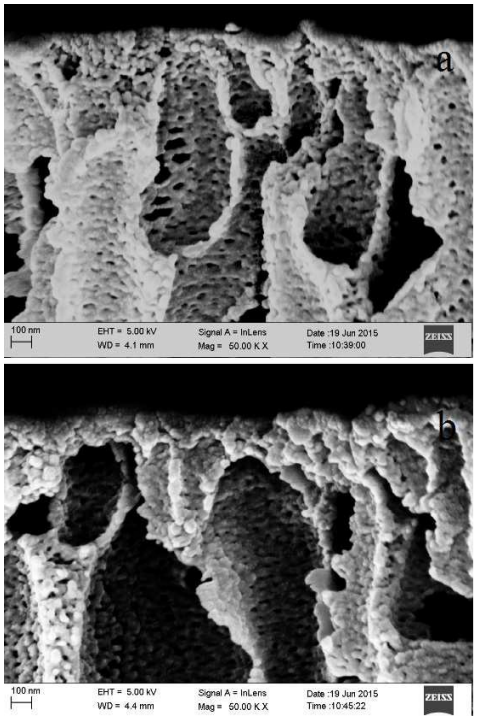

Figure 8 Cross-section FESEM images of (a) original TFC membrane and (b) TFC PDA@ top PSf membrane.

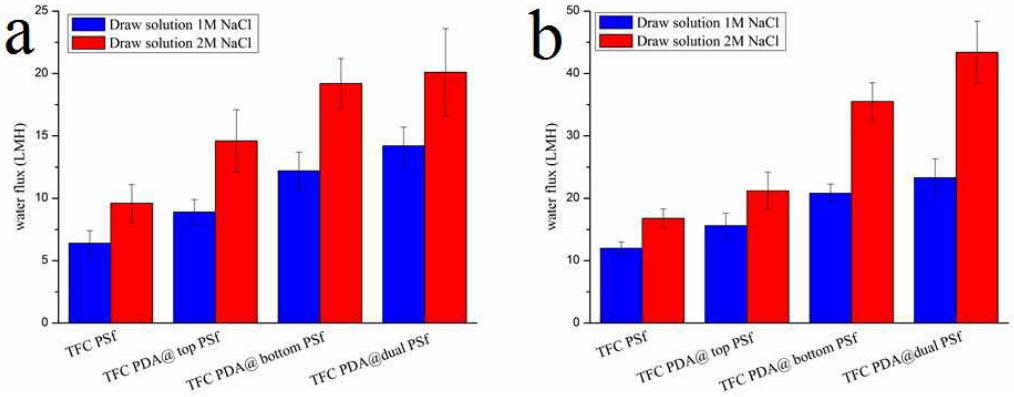

Figure 9 Water fluxes of TFC PSf and TFC PDA modified PSf membranes during FO process, (a) FO mode and (b) PRO mode.

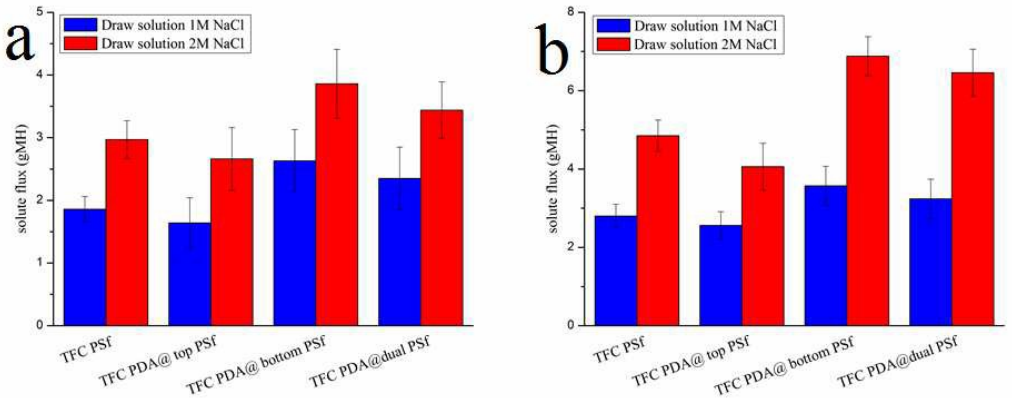

Figure 10 Solute flux of TFC PSf and TFC PDA modified PSf membranes during FO process, (a) FO mode and (b) PRO mode.

Table 1 Surface element compositions of the pristine and modified membranes.

Membrane	Atomic percentage %				O/N	C/N
	O	N	C	S		
PSf	13.62	0	83.36	3.02	-	-
PDA@PSf	19.55	7.84	71.95	0.66	2.49	9.18

Table 2 Surface roughness of TFC-FO membranes.

Membrane	Ra (nm)	Ry (nm)	Rms (nm)
TFC PSf	34.6	288.5	43.4
TFC PDA@ top PSf	52.7	430.4	60.9
TFC PDA@ bottom PSf	35.1	272.6	44.4
TFC PDA@ dual PSf	50.3	398.5	57.3

Ra--Arithmetic mean roughness, Ry--Maximum height, Rms--Square average roughness.

Table 3 Separation properties of membranes prepared with different substrates.

Membrane	Water permeability A (L/m^2 bar h)	Salt permeability B (L/m^2 h)	NaCl rejection (%)
TFC PSf	1.08	0.26	86.5
TFC PDA@ top PSf	1.19	0.22	89.2
TFC PDA@ bottom PSf	1.34	0.50	80.2
TFC PDA@ dual PSf	1.52	0.43	84.0